

Optimising shadow tomography with generalised measurements

H. Chau Nguyen,^{*} Jan Lennart Bönsel,[†] Jonathan Steinberg,[‡] and Otfried Gühne[§]

Naturwissenschaftlich-Technische Fakultät, Universität Siegen,

Walter-Flex-Straße 3, 57068 Siegen, Germany

(Dated: May 19, 2022)

Advances in quantum technology require scalable techniques to efficiently extract information from a quantum system, such as expectation values of observables or its entropy. Traditional tomography is limited to a handful of qubits and shadow tomography has been suggested as a scalable replacement for larger systems. Shadow tomography is conventionally analysed based on outcomes of ideal projective measurements on the system upon application of randomised unitaries. Here, we suggest that shadow tomography can be much more straightforwardly formulated for generalised measurements, or positive operator valued measures. Based on the idea of the least-square estimator, shadow tomography with generalised measurements is both more general and simpler than the traditional formulation with randomisation of unitaries. In particular, this formulation allows us to analyse theoretical aspects of shadow tomography in detail. For example, we provide a detailed study of the implication of symmetries in shadow tomography. Shadow tomography with generalised measurements is also indispensable in realistic implementation of quantum mechanical measurements, when noise is unavoidable. Moreover, we also demonstrate how the optimisation of measurements for shadow tomography tailored toward a particular set of observables can be carried out.

I. INTRODUCTION

Quantum technology is based on our ability to manipulate quantum mechanical states of well-isolated systems: to encode, to process and to extract information from the states of the system. Extracting information in this context means to design and perform measurements on the system so that observables or other properties of the system such as its entropy can be inferred. Naively, one may attempt to perform tomography of the state of the system. This amounts to making a sufficiently large number of different measurements on the system so that the density operator describing the state can be inferred [1–5].

However, when considering how the density operator is used later on, the entire information contained in the density operator is often not needed [6]. In fact, it is impractical to even write down the density operator when the number of qubits is large since the dimension of the many qubit system increases exponentially. In practice, most often one is not interested in the elements of the density operator itself, but rather in certain properties of the quantum state, such as the mean values of certain observables or its entropy. Aiming at inferring directly the observables, bypassing the reconstruction of the density operator, shadow tomography has been theoretically proposed [6]. Huang *et al.* [7] thereafter suggested a practical procedure to realise this aim, which has attracted a lot of attention in the contemporary research of quantum information processing.

The idea of the protocol is simple. Traditionally, quantum state tomography is thought to be only useful once one has accurate enough statistics of measurements. However, state estimators such as the least square estimator can actually be carried out in principle for arbitrary diluted data [8], a fact well established in data science and machine learning [9, 10]. Indeed, a single data point can contribute a noisy estimate of the state; and the final estimated state is obtained by averaging over all the data points. Expectedly, when the data is diluted, the estimated quantum state can be highly noisy and far away from the targeted actual state in the high dimensional state space. This noisy estimation is, however, sufficient to predict certain observables or properties of the quantum states accurately [6, 7]. Crucially, estimation of observables and certain properties of the quantum states for single data points can also be processed without explicitly writing down the density operator [7]. This endows the technique with the promise of scalability.

As for collecting data, Huang *et al.* [7] suggested to perform random unitaries from a certain chosen set of unitaries on the system and perform a standard ideal measurement afterwards. This is equivalent to choosing randomly a measurement from a chosen set of measurements. Since then, various applications of the technique have been found in energy estimation [11, 12], entanglement detection [13], metrology [14], and analysing scrambled data [15], to name a few. Modifications to improve the performance of the scheme and generalisation to channel shadow tomography have also been proposed [16–20]. In this work, we propose a general framework for shadow tomography with so-called generalised measurements (or POVMs). This theoretical framework contains the randomisation of unitaries as a special case, and at the same time allows for analysis of unavailable noise in realistic quantum measurements [21, 22]. To our knowledge, there is so far a single proposed proce-

^{*} chau.nguyen@uni-siegen.de

[†] jan.boensel@uni-siegen.de

[‡] steinberg@physik.uni-siegen.de

[§] otfried.guehne@uni-siegen.de

cedure for shadow tomography with generalised measurements [23]. The suggested procedure is, however, based on the synthesis of the generalised measurement by ideal measurements such that states of the system after the measurement can be assigned. Here we show that this is an unnecessary complication; shadow tomography with generalised measurements can be derived straightforwardly from the least square estimator [8]. In fact, our proposed framework turns out to be much more general and at the same time simpler than randomisation of unitaries. It actually sheds light on many theoretical aspects of shadow tomography.

II. SHADOW TOMOGRAPHY WITH GENERALISED MEASUREMENTS

Consider a quantum system of dimension D , which can either be a single qubit or many qubits. A POVM E on the whole system is described by a positive operator valued measure, that is, a collection of positive operators called effects, $E = \{E_1, E_2, \dots, E_N\}$, normalised by $\sum_{k=1}^N E_k = \mathbb{1}$, where $\mathbb{1}$ denotes the identity operator. Mathematically, a generalised measurement E is the most general way to associate a probability distribution over measurement outcomes to a density operator ρ , i.e., a map $\Phi_E : M_D \rightarrow \mathbb{R}^N$,

$$\Phi_E(\rho) = \{\text{Tr}(\rho E_k)\}_{k=1}^N, \quad (1)$$

where M_D denotes the space of hermitian matrices acting on \mathbb{C}^D . When a single measurement is performed on a system in state ρ , an outcome k is obtained according to these probabilities.

Typical measurements in standard quantum mechanics are a special case of generalised measurements whose effects E_k are projections, thus referred to as *projective measurements*. Moreover, if the projection effects E_k are of rank one, the measurements are called ideal von Neumann measurements, or *ideal measurements* for short. For example, the measurement of a Pauli operator σ_x is an ideal measurement, where the effects are projections on the spin states in the x direction, $\{|x^+\rangle\langle x^+|, |x^-\rangle\langle x^-|\}$. On the other hand, randomising three Pauli measurements $\sigma_x, \sigma_y, \sigma_z$ is equivalent to a generalised measurement with effects being the projections on the spin states in the x, y and z direction, $1/3 \times \{|x^\pm\rangle\langle x^\pm|, |y^\pm\rangle\langle y^\pm|, |z^\pm\rangle\langle z^\pm|\}$, where the prefactor ensures its normalisation (see Appendix B for further discussion). Since these effects form an octahedron on the Bloch sphere, we also refer to it as the octahedron measurement. Generalised measurements, however, allow for much more flexible ways of extracting information from the system. For example, one can consider the generalised measurements defined by different polytopes on the Bloch sphere such as those shown in Fig. 1. Generalised measurements become indispensable in modelling realistic noise in measurement implementation.

Repeating the measurement M times on the system results in a string of outcomes $\{k_i\}_{i=1}^M$. This is the only data based on which the information about the system is drawn. The idea of shadow tomography is to treat the estimate of the density operator as a temporary information processing step so that the properties of the system can be estimated.

Shadow tomography starts with associating a single observation of an outcome k to a distribution $\vec{q}_k = \{\delta_{kl}\}_{l=1}^N$ in \mathbb{R}^N . Such a single data point can be used to obtain a noisy estimate of ρ , called *classical shadow* [24], $\hat{\rho}_k = \chi(\vec{q}_k)$. As a general strategy in data science, one can require the shadow estimator χ to be a least-square estimator [8, 10], of which the solution is well-known (see also Appendix A),

$$\chi_{\text{LS}} = (\Phi_E^\dagger \Phi_E)^{-1} \Phi_E^\dagger. \quad (2)$$

Here we assume that the effects $\{E_k\}_{k=1}^N$ span the whole operator space, in which case E is said to be *informationally complete*, so that $\Phi_E^\dagger \Phi_E$ is invertible. For $\vec{q}_k \in \mathbb{R}^N$ such that $\Phi^\dagger(\vec{q}_k) = E_k$, and if we denote $C_E = \Phi_E^\dagger \Phi_E$, then $C_E(\rho) = \sum_{k=1}^N \text{Tr}(\rho E_k) E_k$. The classical shadow can therefore also be written as

$$\hat{\rho}_k = C_E^{-1}(E_k). \quad (3)$$

Each of the classical shadow serves as an intermediate processed data point for further computation of the observables (see Section III below). Crucially, for an appropriate choice of measurements, the classical shadows $\hat{\rho}_k$ for many-body systems can be efficiently stored and the computation of these observables can be proceeded even without explicitly writing down their matrix elements, which allows for the scalability of the method (see Section VI).

The classical shadow in Eq. (3) resembles that in Ref. [7]. There are however several important differences that we would like to emphasize. Firstly, when the measurement is an ideal measurement, the rank-1 projections E_k are often regarded as the states of the system after the measurement. This may lead to the interpretation that the channel in Eq. (3) estimates the state of the system before the measurement based on its state after the measurement. This interpretation could be however misleading. For a generalised measurement, the effect E_k cannot be interpreted as the state of the system after the measurement. As such, the map C_E^{-1} should not be thought of as acting on the state of the system after the measurement. In fact, our derivation suggests that the state of the system after the measurement is here not important (see Appendix A). Attempts to build classical shadows based on the intuition that E_k is related to the state of the system after the measurement are relatively complicated [19].

Secondly, it is easy to see that over an *infinite* number of runs, the average of the classical shadows converges to ρ , i.e., if $k_i \in \{1, \dots, N\}$ denotes the measurement outcome of the i -th iteration, we have $\lim_{M \rightarrow \infty} \frac{1}{M} \sum_{i=1}^M \hat{\rho}_{k_i} = \rho$. To see

that, one simply notices that in the limit $M \rightarrow \infty$, the sum over empirical data can be replaced by the sum over probability weights $\{\text{Tr}(\rho E_k)\}_{k=1}^N$, that is, $\lim_{M \rightarrow \infty} \frac{1}{M} \sum_{i=1}^M \hat{\rho}_{k_i} = \sum_{k=1}^N \text{Tr}(\rho E_k) \hat{\rho}_k$. The right-hand side is exactly ρ because $C_E[\sum_{k=1}^N \text{Tr}(\rho E_k) \hat{\rho}_k] = \sum_{k=1}^N \text{Tr}(\rho E_k) C_E[C_E^{-1}(E_k)] = C_E(\rho)$ and C_E is invertible. It is important to emphasize, however, that this convergence does *not* guarantee that $C_E^{-1}(E_k)$ is a good estimator [25]. That $C_E^{-1}(E_k)$ is a good estimator is supported by the fact that it is actually the least square estimator.

Lastly, in general, C_E is not trace preserving. Despite converging to the right state upon averaging, the individual classical shadows $\hat{\rho}_k$ are not necessarily unit trace. However, when the measurement is uniform trace, i.e., $\text{Tr}(E_k)$ are the same for all effects E_k , then it is easy to see that C_E is trace-preserving upto a multiplicative factor and all the classical shadows are unit trace. This is often not a restrictive assumption, since starting with a measurement with effects of non-uniform traces, by virtually splitting each effect in an appropriate number of identical smaller effects, a measurement with effects with uniform traces can be achieved [26].

III. ESTIMATION OF OBSERVABLES AND PROPERTIES OF THE QUANTUM STATES – THE SHADOW NORM

Given an observable X , each of the classical shadows $\hat{\rho}_k$ gives an estimate for the mean value $\langle X \rangle$ as $\hat{x}_k = \text{Tr}(\hat{\rho}_k X)$. With the whole dataset $\{k_i\}_{i=1}^M$, the average $1/M \sum_{i=1}^M \hat{\rho}_{k_i}$ converges to ρ , therefore $1/M \sum_{i=1}^M \hat{x}_{k_i}$ converges to $\langle X \rangle$ [7]. In this way, the mean value $\langle X \rangle$ can be estimated. Further refinement using the median-mean estimation was also suggested to reduce the influence of outliers [7].

To understand the convergence of the estimation of an observable X , one considers the variance of the estimator. Given an (unknown) state ρ , the measurement outcomes are randomly distributed according to the distribution $\{\text{Tr}(\rho E_k)\}_{k=1}^N$. This gives rise to the randomly distributed classical shadows $\hat{\rho}_k$ and therefore the estimated mean values $\hat{x}_k = \text{Tr}(\hat{\rho}_k X)$ for $\langle X \rangle$ with probabilities $\{\text{Tr}(\rho E_k)\}_{k=1}^N$. The variance of the estimator \hat{x}_k can then be computed as

$$\text{var}(\hat{x}_k) = \sum_{k=1}^N \text{Tr}(\hat{\rho}_k X)^2 \text{Tr}(\rho E_k) - \langle X \rangle^2. \quad (4)$$

Ignoring the second term results in an upper bound for the variance, and finally assuming the worst case scenario, i.e., maximisation over ρ , one arrives at the definition of the shadow norm of X [7],

$$\text{var}(\hat{x}_k) \leq \|X\|_E^2 = \lambda_{\max}\left\{\sum_{k=1}^N \text{Tr}(\hat{\rho}_k X)^2 E_k\right\}. \quad (5)$$

where $\lambda_{\max}\{\cdot\}$ denotes the maximum of the eigenvalues of the corresponding operator.

Although our analysis in this work also concentrates on the shadow norm (5), one should notice that its definition has a caveat. The shadow norm provides a rigorous bound of the variance of the estimator \hat{x}_k by choosing the state ρ to maximise it. In practice, the targeted state could be very different from this worst case scenario. Therefore, it might also be informative to consider the average of the variance with respect to certain ensemble of states. For example, assuming randomly distributed pure states according to the Haar measure, one can show that up to an additive constant

$$\overline{\|X\|_E^2} \sim \sum_{k=1}^N \text{Tr}(\hat{\rho}_k X)^2 \text{Tr}(E_k) \quad (6)$$

for an observable X normalised with $\text{Tr}(X) = 0$ and $\text{Tr}(X^2) = 1$.

IV. SYMMETRIC GENERALISED MEASUREMENTS AND THE COMPUTATION OF THE CLASSICAL SHADOWS

Crucial for the calculation of classical shadows according to Eq. (3) is the inverse of the channel C_E . It has been observed that for certain classes of measurements, the inverse channel C_E^{-1} is particularly simple [7, 27]. We are to show that behind this simplicity is the symmetry of the generalised measurement, which can be generalised to a much broader class of measurements.

To keep the idea simple, we start with the example of the octahedron generalised measurement over a qubit, leaving the general argument in Appendix C. The effects of this generalised measurement are six effects that are organised on the Bloch sphere as a regular octahedron, see plotted in Fig. 1 (top). Picking a vertex of the octahedron which corresponds to the effect E_k in Fig. 1, we consider the symmetry rotations of the octahedron that leave this vertex invariant. These are rotations by multiples of $\pi/2$ around the axis. Noticeably, there is a single projection (and its complement) that is invariant under these rotations, which corresponds to the state of the spin pointing to the vertex itself, see Fig. 1 (top). In other words, the effect E_k is uniquely specified by the symmetry. One can show that the corresponding classical shadow $\hat{\rho}_k$ is also invariant under these rotations, which then implies that it is a linear combination of E_k and the identity operator $\mathbb{1}$. A quick inspection shows that this property holds for all measurements described by the symmetric solids as plotted in Fig. 1. In fact, this is a general property of the so-called uniform and rigidly symmetric measurements [28], see Appendix C. In this case, one has

$$\hat{\rho}_k = aE_k + b\mathbb{1}. \quad (7)$$

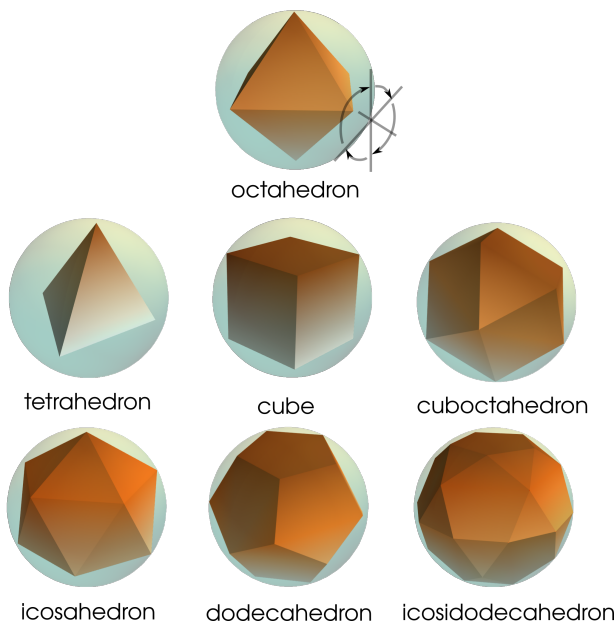


FIG. 1. Symmetric polytopes on the Bloch sphere defining symmetric general measurements with different numbers of effects: octahedron ($N = 6$), tetrahedron ($N = 4$), cube ($N = 8$), cuboctahedron ($N = 12$), icosahedron ($N = 12$), dodecahedron ($N = 20$), icosidodecahedron ($N = 30$). The parameters of the classical shadow a and b in formula (7) are given in Appendix C.

For a qubit ($D = 2$), the coefficients a and b can be explicitly computed, $a = (2\beta - \alpha^2)/(2\gamma - \alpha^3)$ and $b = (\gamma - \alpha\beta)/(2\gamma - \alpha^3)$, where $\alpha = \text{Tr}(E_k)$, $\beta = \text{Tr}(E_k^2)$, and $\gamma = \sum_{l=1}^N \text{Tr}(E_k E_l)^2$ (which are all independent of k). For the more general case of a system of arbitrary dimension D , see Appendix C.

V. EFFECT OF NOISE IN MEASUREMENTS

Most often measurements that are implemented in realistic experimental setups aren't ideal. This is due to various sources of noise in setting up the parameters of the measurement devices, or the resolution and the accuracy of readout signals [21, 22]. To accurately describe these imperfections, generalised measurements must be used.

As an illustrative example, suppose the octahedron measurement is not perfectly implemented so that the measurement effects are not exactly projections onto the spin states, but are mixed with certain white noise. This can be modelled by the effects that are depolarised as

$$1/3 \times \{(1-p)\mathbb{1}/2 + p|t^\pm\rangle\langle t^\pm| : t = x, y, z\}. \quad (8)$$

The classical shadows based on ideal measurements cannot be used in this situation, but our above described framework can. In fact, the measurement is still uniform and rigidly symmetric as long as $p > 0$. The classical

shadows can thus be computed according to Eq. (7) with

$$a(p) = -18p^2/(3 - 6p^2 + p^4), \quad (9)$$

$$b(p) = (3 + p^4)/(6 - 12p^2 + 2p^4). \quad (10)$$

Remarkably, the shadow norm for an *arbitrary* projection onto a spin state is given by $3/2 \times (1 + 1/p^2)$. It is interesting to see that the shadow norm is not very sensitive to noise as $p \approx 1$, but diverges very fast as $p \approx 0$. It is clear that at $p = 0$, the measurement does not reveal any information about the state.

VI. TENSORING THE SHADOW CONSTRUCTION

Shadow tomography is designed for the case where the size of the system is large. Consider the case where the system consists of n qubits, corresponding to the total dimension of $D = 2^n$. In this case, shadow tomography can be performed by making (identical or not identical) generalised measurements $\{E^{(1)}, E^{(2)}, \dots, E^{(n)}\}$ on each of the qubit, each described by a collection of N_i effects, $E^{(i)} = \{E_k^{(i)}\}_{k=1}^{N_i}$. Theoretically, this corresponds to a measurement of a generalised measurement E^{tot} on the whole system with each effect labelled by a string of outcomes $\{k^{(1)}, k^{(2)}, \dots, k^{(n)}\}$,

$$E^{\text{tot}} = E_{k^{(1)}}^{(1)} \otimes E_{k^{(2)}}^{(2)} \otimes \dots \otimes E_{k^{(n)}}^{(n)}. \quad (11)$$

The whole general analysis above can be applied. In fact, such a string of outcomes $\{k^{(1)}, k^{(2)}, \dots, k^{(n)}\}$ corresponds simply to the classical shadow

$$\hat{\rho}^{\text{tot}} = \hat{\rho}_{k^{(1)}}^{(1)} \otimes \hat{\rho}_{k^{(2)}}^{(2)} \otimes \dots \otimes \hat{\rho}_{k^{(n)}}^{(n)}, \quad (12)$$

where $\hat{\rho}_{k^{(i)}}^{(i)} = [C_{E^{(i)}}^{(i)}]^{-1}[E_{k^{(i)}}^{(i)}]$ with $C_{E^{(i)}}^{(i)}$ being the measurement channel for the measurement $E^{(i)}$ on the i -th qubit. This tensoring construction is crucial for the advantage of shadow tomography for large systems. In fact, the typical observables of the system can be easily estimated without explicitly computing the classical shadows in the form of a $D \times D$ matrix [7]. The observable X on the system is typically also of the tensor product form,

$$X = X^{(1)} \otimes X^{(2)} \otimes \dots \otimes X^{(n)}. \quad (13)$$

Then, a single string of outcomes gives rise to the single estimate of $\langle X \rangle$ as

$$\text{Tr}[\hat{\rho}_{k^{(1)}}^{(1)} X^{(1)}] \text{Tr}[\hat{\rho}_{k^{(2)}}^{(2)} X^{(2)}] \dots \text{Tr}[\hat{\rho}_{k^{(n)}}^{(n)} X^{(n)}]. \quad (14)$$

The final estimate of $\langle X \rangle$ is as usual obtained by averaging over all data points. Observe that it is not necessary to construct the large density operator of the whole system of n qubits for this estimation.

If the observable is factorised according to (13), its shadow norm also factorises

$$\|X\|_E = \left\|X^{(1)}\right\|_{E^{(1)}} \left\|X^{(2)}\right\|_{E^{(2)}} \dots \left\|X^{(n)}\right\|_{E^{(n)}}. \quad (15)$$

This in fact also allows the shadow norm to be evaluated and optimised for large systems (see Section VII below.)

VII. OPTIMISATION OF MEASUREMENTS FOR SHADOW TOMOGRAPHY

Given a set of observables $\{X_i\}_{i=1}^m$, one would like to find E so that the maximal shadow norm is minimised,

$$E^* = \arg \min_E \max_i \{\|X_i\|_E\}_{i=1}^m. \quad (16)$$

In our framework, this is an optimisation over the convex domain of generalised measurements. The objective function is, however, nonlinear and therefore heuristic methods are required to carry out the optimisation. We implemented simulated annealing for the minimisation and found the obtained optima to be highly reliable. The following simple example for a single qubit is the basis to understand the case of many qubits.

Example 1 (Optimal generalised measurements for shadow tomography for a qubit). Consider a single qubit. As for the observables, we consider the following possibilities:

(a) Fix the set of observables to be 4 projections corresponding to the 4 effects of the generalised measurement which form the orange regular tetrahedron in Fig. 2 (top left). The squared shadow norm is 2 for the generalised measurement defined exactly by these 4 projections (with an appropriate normalisation factor), and $3/2$ for the octahedron measurement defined by Pauli observables. The optimiser suggests that the tetrahedron generalised measurement obtained by centrally inverted the observables through the centre of the Bloch sphere is optimal with the shadow norm of 1; see the violet tetrahedron in Fig. 2 (top left). Further increasing the number of outcomes does not decrease the obtained shadow norm.

(b) As observables consider the eigenstates of the Pauli observables, which form the octahedron plotted in orange in Fig. 2 (top right). The octahedron measurement formed by these eigenstates themselves gives the squared shadow norm of $3/2$. Interestingly, the optimiser shows that the squared shadow norm of $3/2$ can also be obtained with the tetrahedron generalised measurement of 4 outcomes oriented as indicated by the violet tetrahedron in Fig. 2 (top right). Further increasing the number of outcomes does not decrease the obtained shadow norm.

(c) Lastly we consider the set of a varying number of observables which are random projections distributed according to the Haar measure on the Bloch sphere. Fig. 2 (bottom) presents the shadow norms obtained by the optimiser with respect to the number of observables. For small number of observables ($m \leq 15$), the optimiser always finds measurements with a given number of outcomes significantly better than the standard tetrahedron ($N = 4$) or the octahedron measurements ($N = 6$). It is interesting to notice that for 4-outcome measurements, the found optimal value of the shadow norm converges slowly to the tetrahedron measurement reaching the squared shadow norm of 2 as the number of observable increases. On the other hand, if the number of outcome is fixed to be 6 or 8, the shadow norm con-

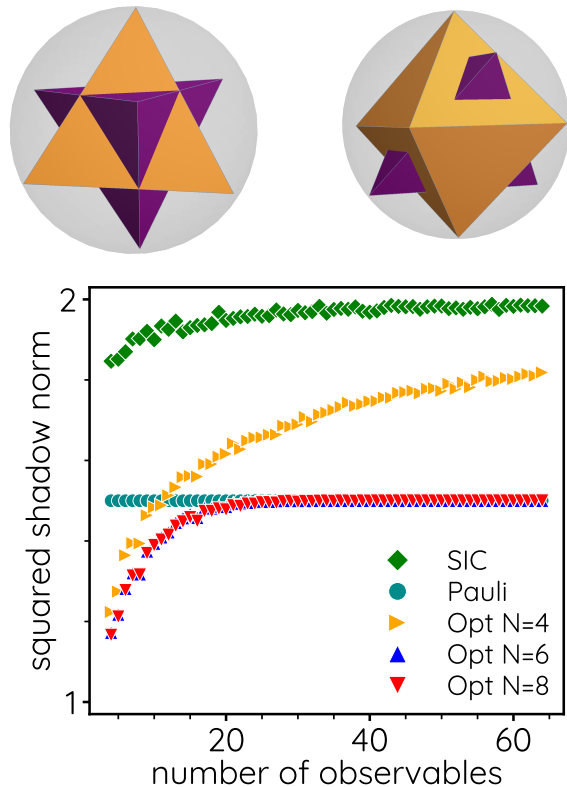


FIG. 2. Targeted observables and optimal generalised measurements. (top left) Observables correspond to four projections of a tetrahedron generalised measurement and the effects of the optimal measurement is the tetrahedron measurement which is centrally inverted. (top right) The projection onto the eigenstates of the Pauli observables σ_x , σ_y and σ_z forming the orange octahedron, and the optimal measurement is also the tetrahedron measurement with vertices oriented along the four vertices of the violet tetrahedron. (bottom) Minimal shadow norms given by the optimiser (labeled Opt with the number of measurement outcomes) as a function of the number of projection observables randomly distributed according to the Haar measure together with that for other generalised measurements.

verges rather quickly to the octahedron measurement with squared shadow norm of $3/2$.

The last example (c) hints that if the targeted observables are all the projections on arbitrary states of the qubit, the optimal measurement would be the octahedron measurement. This can indeed be demonstrated for measurements with uniform trace, see Appendix D.

For many qubits, the exhaustive optimisation procedure as described above becomes quickly infeasible because the number of parameters increases exponentially. We can however assume that for a many-qubit system, the generalised measurement is factorised in the form (11). Moreover, it is also natural to consider only measurements which are identical over the qubits, that is, $E^{(1)} = E^{(2)} = \dots = E^{(n)}$. This is practically convenient, but also reasonable if the qubits in the system

are equivalent. The complexity of the computation under these assumptions is only linear in the number of qubits and the number of observables. This makes the study of the optimal measurements for shadow tomography of relatively large systems of qubits possible.

Example 2 (Optimal uniform factorised generalised measurements for shadow tomography). We consider a system of 60 qubits. As for the set of observables, we choose 60 observables which are products of different component observables on single qubits. The component observables on single qubits are sampled from (i) the four effects of the tetrahedron measurement as described in Example 1, and (ii) projections randomly distributed according to the Haar measure. As the qubits are equivalent, one might anticipate that the optimal factorising measurement for the qubits is similar to those that are optimised separately for each qubit. Our simulations confirm this expectation. In case (i), we again recover the inverted tetrahedron measurement as the typical optimal choice of measurement, in accordance to Example 1 (a). In case (ii), we find that the octahedron measurement is almost always found to be very close to optimality, also supported by results in Example 1 (b).

As we already remarked above, the shadow norm is a rigorous bound on the worst case scenario, which may be very different from the actual state of the system in reality. For example, our simulation of the estimation of the mean values and correlations of the transverse Ising model using shadow tomography shows that there is little difference between the octahedron measurement or the tetrahedron measurement. Optimising measurements under the prior knowledge of the targeted state would be an interesting option for future work.

VIII. CONCLUSION

We have formulated shadow tomography with generalised measurements using the least square state estimation. Being both more general and simpler, the formulation allows us to analyse various theoretical aspects of shadow tomography, such as the implication of symmetry and the optimisation of the experimental setup. This also opens a range of interesting questions for future research. For example, extension of this framework to channel tomography would be of direct interest. It would be also important to see whether the technique of derandomisation [16] can also be incorporated in this general framework. Also the extension of the construction of optimal measurements for observables to the estimation of entropy is a very interesting research direction.

ACKNOWLEDGMENTS

The authors would like to thank Satoya Imai, Matthias Kleinmann, Zhen-Peng Xu, and Benjamin Yadin for inspiring discussions. The University of Siegen is kindly

acknowledged for enabling our computations through the OMNI cluster. This work was supported by the Deutsche Forschungsgemeinschaft (DFG, German Research Foundation, project numbers 447948357 and 440958198), the Sino-German Center for Research Promotion (Project M-0294), and the ERC (Consolidator Grant 683107/TempoQ). JLB and JS acknowledge support from the House of Young Talents of the University of Siegen.

Appendix A: Least square derivation of shadow tomography with generalised measurements

The derivation of the solution to the least square problem is standard in data science and machine learning literature [10], which has also been used in the theory of quantum tomography, see e.g., Ref. [8]. For a self-contained complete understanding of the logic, we present here the derivation specifically for shadow tomography.

Recall that a measurement $E = \{E_k\}_{k=1}^N$ is associated with a map Φ_E which maps ρ to a probability distribution, $\Phi_E : M_D \rightarrow \mathbb{R}^N$, $\Phi_E(\rho) = \{\text{Tr}(\rho E_k)\}_{k=1}^N$. An unbiased linear estimator for ρ is a map $\chi : \mathbb{R}^N \rightarrow M_D$ which maps a probability distribution to a quantum state such that $(\chi \circ \Phi_E)$ acts as identity over M_D . That means, as long as the statistics $\Phi_E(\rho)$ of a state ρ can be exactly measured, χ allows for an exact construction of the state ρ . Note that if $\{E_k\}_{k=1}^N$ form a basis for the operator space, that is, E is informationally complete, but not overcomplete, then Φ_E is invertible and $\chi = \Phi_E^{-1}$. In the case that E is informationally *overcomplete*, χ is not uniquely defined. In fact, Φ_E is not surjective in this case: there are probability distributions in \mathbb{R}^N that give rise to no state ρ . In this situation, the natural choice is the least square estimator, namely, for a distribution $\vec{p} \in \mathbb{R}^N$, the estimated state is defined by

$$\chi_{\text{LS}}(\vec{p}) = \arg \min_{\tau} L(\tau), \quad (\text{A1})$$

where

$$L(\tau) = \sum_{i=1}^N [\text{Tr}(\tau E_i) - p_i]^2. \quad (\text{A2})$$

To carry out this minimisation, we consider the expansion of $L(\tau + \delta\tau)$ in the first order of the small variation $\delta\tau$ of τ ,

$$\delta L = 2 \sum_{i=1}^N [\text{Tr}(\tau E_i) - p_i] \text{Tr}(E_i \delta\tau). \quad (\text{A3})$$

That L is minimised implies that $\delta L = 0$ for all choices of $\delta\tau$. It must then hold that

$$\sum_{i=1}^N [\text{Tr}(\tau E_i) - p_i] E_i = 0. \quad (\text{A4})$$

Using the definition of Φ_E , one can rewrite the above equation as

$$\Phi_E^\dagger[\Phi_E(\tau) - \vec{p}] = 0. \quad (\text{A5})$$

The solution of the estimator $\chi_{\text{LS}}(\vec{p})$ can be found to be

$$\chi_{\text{LS}} = (\Phi_E^\dagger \Phi_E)^{-1} \Phi_E^\dagger. \quad (\text{A6})$$

Observe that when Φ_E is invertible, $\chi_{\text{LS}} = \Phi_E^{-1}$.

This procedure gives the exact reconstruction of ρ as long as the exact (thus valid) statistics \vec{p} for the measurement outcomes is available. Remarkably this estimator is linear, which implies that the estimated state over the whole data set can be split into the sum of the estimated states for the single data points. Indeed, a single observation of an outcome k can be associated with an elementary statistics vector $\vec{q}_k = \{\delta_{ki}\}_{i=1}^N \in \mathbb{R}^N$. The statistics of the whole dataset of a string of outcomes $\{k_i\}_{i=1}^M$ is given by

$$\vec{p} = \frac{1}{M} \sum_{i=1}^M \vec{q}_{k_i}, \quad (\text{A7})$$

and therefore

$$\chi_{\text{LS}}(\vec{p}) = \frac{1}{M} \sum_{i=1}^M \chi_{\text{LS}}(\vec{q}_{k_i}). \quad (\text{A8})$$

One can then confirm that $\chi_{\text{LS}}(\vec{q}_{k_i})$ is exactly the classical shadow corresponding to the outcome k_i as given in Eq. (3).

The linearity of the estimator is crucial to shadow tomography. For instance, this allows one to estimate linear observables with single data points and later on average over the whole dataset. Although in the low sampling regime, $M \ll D$, the estimated state can be far from the targeted state in the state space, it can be sufficient to estimate many linear observables [6, 7]. The name (classical) shadow tomography reflects the fact that we are not aiming at reconstructing the density operator of the system, but only the classical values of observables [6]. For more on the rationale and detailed theory behind, we refer the readers to Ref. [6] and the references therein.

Appendix B: Relation to randomised ideal measurements

The often used scheme of randomised ideal projective measurements as described in Ref. [7] can be considered as a special realisation of a generalised measurement. Specifically, following Ref. [7], a random unitary U is drawn from a selected set \mathcal{U} of unitaries and carried out on the system before making the measurement in a standard basis $\{|b\rangle\}_{b=1}^D$ (such as the computational basis). This corresponds to the random projective measurement in the basis $\{U^\dagger |b\rangle\}_{b=1}^D$. Then the whole procedure effectively simulates a generalised measurement with effects

$\{1/|\mathcal{U}| U^\dagger |b\rangle\langle b| U : U \in \mathcal{U}, b = 1, 2, \dots, D\}$, where $|\mathcal{U}|$ is the total number of unitaries in \mathcal{U} . Mathematically, the resulted generalised measurement is a convex combination of the ideal measurement in the chosen ideal measurements. This is a well-known method of simulating generalised measurements with ideal ones, known as preprocessing [29].

Our suggested scheme of implementing shadow tomography using a single generalised measurement brings several interesting new perspectives. Firstly, the randomised unitary description is heavily over parametrised, i.e., having much more parameters than necessary. For example, the unitary ensemble of the Clifford group on a qubit contains 24 elements, and yet is equivalent to a single generalised measurement of 6 outcomes corresponding to six directions of the three standard axes, $1/3 \times \{|x^\pm\rangle\langle x^\pm|, |y^\pm\rangle\langle y^\pm|, |z^\pm\rangle\langle z^\pm|\}$. This over parametrisation makes it difficult to keep track over the parameters and to optimise the procedure. Furthermore, the same generalised measurement can be simulated with different sets of unitaries and there are also generalised measurements that cannot be simulated by unitary ensembles (such as the tetrahedron measurement discussed in the main text) [30]. With all these difficulties, finding an optimal set of unitaries for shadow tomography appears to be intractable, even for the simplest case of a single qubit. As we have showed in the main text, using generalised measurements, the problem of optimising shadow tomography turns out to be possible.

Using generalised measurements also brings a new perspective on the implementation of the procedure. A generalised measurement can be implemented by a measurement on the ancillary system after an appropriate coupling to the objective system. While this can still be challenging in practice, it avoids changing measurement settings which require frequent (re)calibration of the setup.

Appendix C: Symmetry of generalised measurements and the computation of classical shadows

In the appendix, we describe how the symmetry of a generalised measurement can be analysed and how the formula for the classical shadow can be drawn just from the consideration of symmetry. We say that a measurement $E = (E_1, E_2, \dots, E_N)$ is symmetric if there is a subgroup G of the permutation group over $(1, 2, \dots, N)$ and a representation $U : G \rightarrow U(D)$ such that $E_{g(k)} = U_g E_k U_{g^{-1}}$. One can easily show that if E is symmetric under G , then also $\Phi_E : M_D \rightarrow \mathbb{R}^N$ is covariant under G , that is, $\Phi_E(U_g \rho U_{g^{-1}}) = g[\Phi_E(\rho)]$, where g acts on a probability distribution \vec{p} by $[g(\vec{p})]_k = p_{g^{-1}(k)}$. As a consequence, Φ_E^\dagger is covariant under G , i.e., $\Phi_E^\dagger[g(\vec{p})] = U_g \Phi_E^\dagger(\vec{p}) U_{g^{-1}}$ for all distribution \vec{p} . This in turn implies that $C_E = \Phi_E^\dagger \Phi_E$ and particularly its inverse C_E^{-1} are also covariant under G , $C_E^{-1}(U_g X U_{g^{-1}}) =$

$U_g C_E^{-1}(X) U_{g^{-1}}$ for all hermitian operators X .

We consider the case that E is uniform, which means G acts transitively on the outcomes, or in other words any effect can be mapped to another effect. In particular, this implies that $\text{Tr}(E_k)$ is independent of k , and we denote $\alpha = \text{Tr}(E_k)$. Following Ref. [28], we consider the stabiliser subgroup G_k over k , that is, the subgroup of G that leaves k invariant. Since G_k leaves k invariant, E_k commutes with $U(G_k)$. Because C_E^{-1} is covariant under G , it is clear that $\hat{\rho}_k = C_E^{-1}(E_k)$ also commutes with $U(G_k)$. One says that E is rigidly symmetric [28] if the representation U restricted to any stabiliser subgroup over k , G_k , has exactly two irreducible representations. This is the characterisation of the property that, an operator commuting with $U(G_k)$ can only be a linear combination of E_k and $\mathbb{1}$. Hence if E is rigidly symmetric, then

$$\hat{\rho}_k = aE_k + b\mathbb{1}. \quad (\text{C1})$$

To compute a and b , one notice that $C_E(\hat{\rho}_k) = a \sum_{l=1}^N \text{Tr}(E_k E_l) E_l + b\alpha\mathbb{1}$, which is identified with E_k . Taking the trace of this equation and the trace of it after multiplying the two sides with E_k , one obtains

$$\alpha = a\alpha^2 + b\alpha D, \quad (\text{C2})$$

$$\beta = a\gamma + b\alpha^2, \quad (\text{C3})$$

with $\beta = \text{Tr}(E_k^2)$, $\gamma = \sum_{l=1}^N \text{Tr}(E_k E_l)^2$, both independent of k due to the uniformity. The coefficients a and b can be then explicitly solved,

$$a = (D\beta - \alpha^2)/(D\gamma - \alpha^3), \quad (\text{C4})$$

$$b = (\gamma - \alpha\beta)/(D\gamma - \alpha^3). \quad (\text{C5})$$

A large class of uniform and rigidly symmetric measurements beyond qubits are studied in Ref. [28], whose parameters of the classical shadows are enumerated in Table I.

Appendix D: Proof of the optimality of octahedron measurement for shadow tomography

For a pure state $|\lambda\rangle$, we use P_λ to denote the associated projection $P_\lambda = |\lambda\rangle\langle\lambda|$. We consider the problem of predicting all the expectation values of these projections based on classical shadows generated by a measurement E . We characterise the predicting power of the shadow tomography by the maximal shadow norm among all these projections,

$$\max_{\lambda} \|P_\lambda\|_E^2 = \max_{\lambda} \max_{\rho} \sum_{k=1}^N \langle\lambda|\rho_k|\lambda\rangle^2 \text{Tr}[\rho E_k]. \quad (\text{D1})$$

We are to show that the octahedron measurement is optimal in the sense that it minimises this maximal shadow norm. We assume that the measurement has uniform

d	ST	$ M $	Comments	a	b
2	8	6	Octahedron	9	-1
		8	Cube	12	-1
		12	Cuboctahedron	18	-1
	16	12	Icosahedron	18	-1
		20	Dodecahedron	30	-1
3	24	21		28	-1
		12	csMUB	16	-1
	27	45		60	-1
		60		80	-1
	4	28	12	Real MUB	9
20			csMUB	25	-1
29		40		50	-1
		80		100	-1
30		300		225	$-\frac{1}{2}$
31		60		75	-1
	480		600	-1	

TABLE I. Parameters for the inverse of the measurement channels for symmetric generalised measurements constructed in Ref. [28] with the same naming convention. Notice that here each row corresponds to a single generalised measurement, which is decomposed to several idealised measurements in Ref. [28]. The latter information can be used to simulate the indicated generalised measurement by randomising the corresponding group of idealised measurements.

trace. This implies that ρ_k are all unit trace. In fact, we can derive an explicit formula for the classical shadows in the Bloch representation.

Using the Pauli matrices $\{\sigma_i\}_{i=1}^4 = \{\mathbb{1}, \sigma_x, \sigma_y, \sigma_z\}$ as a basis for the operator space, an operator X on the qubit can be identified with a real vector of 4 components, $X = \frac{1}{2} \sum_{i=1}^4 x_i \sigma_i$, where $x_i = \text{Tr}(\rho \sigma_i)$. Notice that for two operators X and Y , which are presented by two vectors x and y respectively, $\text{Tr}(XY) = \frac{1}{2} \sum_{i=1}^4 x_i y_i$. Also, the identity operator $\mathbb{1}$ is identified with the vector $(2, 0, 0, 0)^T$.

In this Bloch representation, each of the effects E_k can be represented by a vector of the form $\frac{2}{N} \begin{pmatrix} 1 \\ \vec{r}_k \end{pmatrix}$, where $\|\vec{r}_k\| \leq 1$ and $\sum_{k=1}^N \vec{r}_k = 0$. Therefore

$$\Phi_E^\dagger = \frac{2}{N} \begin{pmatrix} 1 & 1 & \cdots & 1 \\ \vec{r}_1 & \vec{r}_2 & \cdots & \vec{r}_N \end{pmatrix}. \quad (\text{D2})$$

And the map Φ_E can be identified with the matrix

$$\Phi_E = \frac{1}{N} \begin{pmatrix} 1 & \vec{r}_1 \\ 1 & \vec{r}_2 \\ \cdot & \cdot \\ 1 & \vec{r}_N \end{pmatrix}. \quad (\text{D3})$$

Explicit calculation then shows that

$$\chi = \begin{pmatrix} 1 & 1 & \cdots & 1 \\ H^{-1}\vec{r}_1 & H^{-1}\vec{r}_2 & \cdots & H^{-1}\vec{r}_N \end{pmatrix}, \quad (\text{D4})$$

where

$$H = \frac{1}{N} \sum_{k=1}^N \vec{r}_k \vec{r}_k^T. \quad (\text{D5})$$

Notice that by definition the columns of χ are exactly ρ_k in the Bloch representation. The explicit formula for the classical shadow allows us to explicitly estimate the shadow norm.

Let us now turn back to the maximal shadow norm (D1). Taking the particular choice of $\rho = |\lambda\rangle\langle\lambda|$ as an ansatz, we have a lower bound

$$\max_{\lambda} \|P_{\lambda}\|_E^2 \geq \max_{\lambda} \sum_{k=1}^N \langle\lambda|\rho_k|\lambda\rangle^2 \langle\lambda|E_k|\lambda\rangle. \quad (\text{D6})$$

Then replacing the maximum over λ by the average over the Haar measure ω on the Bloch sphere, one obtains the further lower bound

$$\max_{\lambda} \|P_{\lambda}\|_E^2 \geq \int d\omega(\lambda) \sum_{k=1}^N \text{Tr}[(\rho_k \otimes \rho_k \otimes E_k) P_{\lambda}^{\otimes 3}]. \quad (\text{D7})$$

It is easy to show that [31]

$$\int d\omega(\lambda) P_{\lambda}^{\otimes 3} = \frac{1}{12} [(1, 2) + (2, 3) + (3, 1)], \quad (\text{D8})$$

where (1, 2), (2, 3) and (3, 1) denote the operators that permute the corresponding tensor terms in $(\mathbb{C}^2)^{\otimes 3}$. We then arrive at

$$\max_{\lambda} \|P_{\lambda}\|_E^2 \geq \frac{1}{12} \sum_{k=1}^N [\text{Tr}(\rho_k^2) \text{Tr}(E_k) + 2 \text{Tr}(\rho_k) \text{Tr}(\rho_k E_k)], \quad (\text{D9})$$

where we have used

$$\begin{aligned} \text{Tr}[(\rho_k \otimes \rho_k \otimes E_k)(1, 2)] &= \text{Tr}(\rho_k^2) \text{Tr}(E_k), \\ \text{Tr}[(\rho_k \otimes \rho_k \otimes E_k)(2, 3)] &= \text{Tr}(\rho_k) \text{Tr}(\rho_k E_k), \\ \text{Tr}[(\rho_k \otimes \rho_k \otimes E_k)(3, 1)] &= \text{Tr}(\rho_k) \text{Tr}(\rho_k E_k). \end{aligned} \quad (\text{D10})$$

Using the explicit Bloch representation for E_k and ρ_k , we obtain

$$\max_{\lambda} \|P_{\lambda}\|_E^2 \geq \frac{1}{12} \left[3 + \frac{1}{N} \sum_{k=1}^N (\vec{r}_k^T H^{-2} \vec{r}_k + 2 \vec{r}_k^T H^{-1} \vec{r}_k) \right]. \quad (\text{D11})$$

Notice that

$$\begin{aligned} \frac{1}{N} \sum_{k=1}^N \vec{r}_k^T H^{-1} \vec{r}_k &= \frac{1}{N} \sum_{k=1}^N \text{Tr}(H^{-1} \vec{r}_k \vec{r}_k^T) \\ &= \text{Tr}(H^{-1} H) \\ &= 3, \end{aligned}$$

and similarly

$$\frac{1}{N} \sum_{k=1}^N \vec{r}_k^T H^{-2} \vec{r}_k = \text{Tr}(H^{-1}).$$

Then

$$\max_{\lambda} \|P_{\lambda}\|_E^2 \geq \frac{1}{12} [9 + \text{Tr}(H^{-1})]. \quad (\text{D12})$$

Notice that H is positive and denote its positive eigenvalues by t_1 , t_2 and t_3 , then $\text{Tr}(H^{-1}) = 1/t_1 + 1/t_2 + 1/t_3 \geq 9/(t_1 + t_2 + t_3) = 9/\text{Tr}(H)$. Moreover, $\text{Tr}(H) = 1/N \sum_{k=1}^N \vec{r}_k^T \vec{r}_k \leq 1$. We then arrive at

$$\max_{\lambda} \|P_{\lambda}\|_E^2 \geq \frac{3}{2}. \quad (\text{D13})$$

By direct calculation, one can then show that this inequality is saturated for the octahedron measurement (in which case, H is $1/3$ of the identity matrix). This demonstrates that the octahedron measurement is an optimal choice for the chosen set of observables.

-
- [1] D. T. Smithey, M. Beck, M. G. Raymer, and A. Faridani, “Measurement of the Wigner distribution and the density matrix of a light mode using optical homodyne tomography: Application to squeezed states and the vacuum,” *Phys. Rev. Lett.* **70**, 1244 (1993).
- [2] D. F. V. James, P. G. Kwiat, W. J. Munro, and A. G. White, “Measurement of qubits,” *Phys. Rev. A* **64**, 052312 (2001).
- [3] H. Häffner, W. Hänsel, C. F. Roos, J. Benhelm, D. Chekhlov, M. Chwalla, T. Körber, U. D. Rapol, M. Riebe, P. O. Schmidt, C. Becher, O. Gühne, W. Dür, and R. Blatt, “Scalable multiparticle entanglement of trapped ions,” *Nature* **438**, 643–646 (2005).
- [4] C. Schwemmer, L. Knips, D. Richart, H. Weinfurter, T. Moroder, M. Kleinmann, and O. Gühne, “Systematic errors in current quantum state tomography tools,” *Phys. Rev. Lett.* **114**, 080403 (2015).
- [5] M. Paris and J. Řeháček, *Quantum State Estimation* (Springer, Berlin, Heidelberg, 2004).
- [6] S. Aaronson, “Shadow tomography of quantum states,” *arXiv:1711.01053* (2018).
- [7] H. Y. Huang, R. Kueng, and J. Preskill, “Predicting many properties of a quantum system from very few measurements,” *Nat. Phys.* **16**, 1050–1057 (2020).
- [8] M. Guță, J. Kahn, R. Kueng, and J. A. Tropp, “Fast state tomography with optimal error bounds,” *J. Phys.*

- A: *Math. Theor.* **53**, 204001 (2020).
- [9] P. Mehta, M. Bukov, C.-H. Wang, A. G. R. Day, C. Richardson, C. K. Fisher, and D. J. Schwab, “A high-bias, low-variance introduction to machine learning for physicists,” *Phys. Rep.* **810**, 1–124 (2019).
- [10] C. M. Bishop, *Pattern Recognition and Machine Learning* (Springer New York, 2006).
- [11] C. Hadfield, “Adaptive Pauli shadows for energy estimation,” [arXiv:2105.12207](https://arxiv.org/abs/2105.12207) (2021).
- [12] C. Hadfield, S. Bravyi, R. Raymond, and A. Mezzacapo, “Measurements of quantum Hamiltonians with locally-biased classical shadows,” [arXiv:2006.15788](https://arxiv.org/abs/2006.15788) (2020).
- [13] A. Neven, J. Carrasco, V. Vitale, C. Kokail, A. Elben, M. Dalmonte, P. Calabrese, P. Zoller, B. Vermersch, R. Kueng, and B. Kraus, “Symmetry-resolved entanglement detection using partial transpose moments,” *npj Quantum Inf.* **7**, 1–12 (2021).
- [14] A. Rath, C. Branciard, A. Minguzzi, and B. Vermersch, “Quantum fisher information from randomized measurements,” *Phys. Rev. Lett.* **127**, 260501 (2021).
- [15] R. J. Garcia, Y. Zhou, and A. Jaffe, “Quantum scrambling with classical shadows,” *Phys. Rev. Research* **3**, 033155 (2021).
- [16] H. Y. Huang, R. Kueng, and J. Preskill, “Efficient estimation of pauli observables by derandomization,” *Phys. Rev. Lett.* **127**, 030503 (2021).
- [17] A. Elben, R. Kueng, H. Y. Huang, R. van Bijnen, C. Kokail, M. Dalmonte, P. Calabrese, B. Kraus, J. Preskill, P. Zoller, and B. Vermersch, “Mixed-state entanglement from local randomized measurements,” *Phys. Rev. Lett.* **125**, 200501 (2020).
- [18] L. K. Joshi, A. Elben, A. Vikram, B. Vermersch, V. Galitski, and P. Zoller, “Probing many-body quantum chaos with quantum simulators,” *Phys. Rev. X* **12**, 011018 (2022).
- [19] R. Levy, D. Luo, and B. K. Clark, “Classical shadows for quantum process tomography on near-term quantum computers,” [arXiv:2110.02965](https://arxiv.org/abs/2110.02965) (2021).
- [20] J. Helsen, M. Ioannous, I. Roth, J. Kitzinger, E. Onorati, A. H. Werner, and J. Eisert, “Estimating gate-set properties from random sequences,” [arXiv:2110.13178](https://arxiv.org/abs/2110.13178) (2021), [arXiv: 2110.13178](https://arxiv.org/abs/2110.13178).
- [21] F. Arute, K. Arya, R. Babbush *et al.*, “Quantum supremacy using a programmable superconducting processor,” *Nature* **574**, 505–510 (2019).
- [22] Y. Chen, M. Farahzad, S. Yoo, and T.-C. Wei, “Detector tomography on IBM quantum computers and mitigation of an imperfect measurement,” *Phys. Rev. A* **100**, 052315 (2019).
- [23] A. Acharya, S. Saha, and A. M. Sengupta, “Informationally complete POVM-based shadow tomography,” [arXiv:2105.05992](https://arxiv.org/abs/2105.05992) (2021).
- [24] This terminology is suggested in Ref. [7]. Notice that the original meaning of shadow tomography in Ref. [6] is slightly different.
- [25] In fact, the above proof of convergence holds true if C_E is replaced by any invertible channel $\tilde{C}_E(\rho) = \sum_{k=1}^N \text{Tr}(\rho E_k) \tau_k$ for arbitrary operators τ_k . This once more highlights that one should not associate E_k with the state of the system after the measurements.
- [26] Suppose E is a measurement with difference traces for each effect, $\alpha_k = \text{Tr}(E_k)$. One can always approximate α_k by a rational number. Then one can choose a sufficient small number ϵ such that $\alpha_k/\epsilon = N_k$ are all integers. Then we split an effect E_k into N_k identical effects $(E_k/N_k, E_k/N_k, \dots, E_k/N_k)$ and obtain a new measurement of $\sum_{k=1}^N N_k$ effects. This measurement is uniform trace by construction.
- [27] K. Bu, D. E. Koh, R. J. Garcia, and A. Jaffe, “Classical shadows with Pauli-invariant unitary ensembles,” [arXiv:2202.03272](https://arxiv.org/abs/2202.03272) (2022).
- [28] H. C. Nguyen, S. Designolle, M. Barakat, and O. Gühne, “Symmetries between measurements in quantum mechanics,” [arXiv:2003.12553](https://arxiv.org/abs/2003.12553) (2020).
- [29] T. Heinosaari and M. Ziman, *The Mathematical Language of Quantum Theory: From Uncertainty to Entanglement* (Cambridge University Press, 2012).
- [30] G. M. D’Ariano, P. Lo Presti, and P. Perinotti, “Classical randomness in quantum measurements,” *J. Phys. A: Math. Gen.* **38**, 5979–5991 (2005).
- [31] W. Fulton and J. Harris, *Representation Theory* (Springer New York, 2004).